Molecular Therapy
Methods & Clinical Development
Original Article

Detection of mutant antigen-specific T cell receptors against multiple myeloma for T cell engineering

Masahiro Okada,[1] Kanako Shimizu,[1] Hiroshi Nakazato,[1] Satoru Yamasaki,[1] and Shin-ichiro Fujii[1,2]

[1]Laboratory for Immunotherapy, RIKEN Center for Integrative Medical Sciences, 1-7-22, Suehiro-cho, Tsurumi-ku, Yokohama, Kanagawa 230-0045, Japan; [2]RIKEN Program for Drug Discovery and Medical Technology Platforms, RIKEN, 1-7-22, Suehiro-cho, Tsurumi-ku, Yokohama, Kanagawa 230-0045, Japan

Multiple myeloma (MM) remains an incurable hematological neoplasm. Neoantigen-specific T cell receptor (TCR)-engineered T (TCR-T) cell therapy is a potential alternative treatment. Particularly, TCRs derived from a third-party donor may cover broad ranges of neoantigens, whereas TCRs in patients suffering from immune disorders are limited. However, the efficacy and feasibility of treating MM have not been evaluated thoroughly. In this study, we established a system for identifying immunogenic mutant antigens on MM cells and their corresponding TCRs using healthy donor-derived peripheral blood mononuclear cells (PBMCs). Initially, the immune responses to 35 candidate peptides predicted by the immunogenomic analysis were investigated. Peptide-reactive T lymphocytes were enriched, and subsequently, TCR repertoires were determined by single-cell TCR sequencing. Eleven reconstituted TCRs showed mutation-specific responses against 4 peptides. Particularly, we verified the HLA-A*24:02-binding QYSPVQATF peptide derived from COASY S55Y as the naturally processed epitope across MM cells, making it a promising immune target. Corresponding TCRs specifically recognized COASY S55Y^{+}HLA-A*24:02^{+} MM cells and augmented tumoricidal activity. Finally, adoptive cell transfer of TCR-T cells showed objective responses in the xenograft model. We initiatively proposed the utility of tumor mutated antigen-specific TCR genes to suppress MM. Our unique strategy will facilitate further identification of neoantigen-specific TCRs.

INTRODUCTION

Durable immune checkpoint blockade (ICB) responses observed in many tumor patients, particularly those with higher tumor mutation burden or microsatellite instability, drastically verified the clinical value of neoantigens in tumor immunotherapy.[1,2] Tumor neoantigens derived from somatic mutations, which possess non-self antigenicity and tumor specificity, are the ideal immune targets. Considering that neoantigen-specific immune responses are well observed in ICB responders,[3,4] direct neoantigen targeting holds promise as a rational strategy for cancer treatment. Vaccines using neoantigens elicit objective responses in many patients with tumors.[5] Furthermore, adoptive cell transfer of tumor-infiltrating lymphocytes (TILs) achieves considerable tumor regression by targeting patient-specific neoantigens.[6–8] However, the curative responses to neoantigen vaccines or TIL infusion partly depend on the precondition of patients' immunity. Hence, neoantigen-specific T cell receptor (TCR)-engineered T (TCR-T) cells, which have specific cytotoxicity against tumors, are a potentially versatile treatment for patients with solid and hematological tumors.[9,10]

Multiple myeloma (MM) is a hematological malignancy caused by aggressive proliferation of plasma cells in the bone marrow, presenting systemic clinical symptoms such as severe bone fractures, anemia, immunodeficiency, and renal failure.[11,12] The incidence rate of MM increases yearly, accounting for the second highest among hematological neoplasms.[13] Over the past few decades, in addition to autologous hematopoietic stem cell transplantation (ASCT), chemical compounds, such as immunomodulatory drugs and proteasome inhibitors, and immunotherapies, such as monoclonal antibodies or chimeric antigen receptor (CAR)-T cell therapy, targeting CD38 or BCMA have been clinically applied. These advances could improve therapy for MM.[14] However, it largely remains an incurable disease because of its high recurrence rate.[15,16] Because patients with relapsed MM who are resistant to conventional treatments show poor prognoses, development of alternative therapeutic strategies is imperative.

Neoantigens in patients with MM have been demonstrated recently to be targets by host immunity, particularly after ASCT or ICB treatment.[17] In current regimens for MM, however, the neoantigen burden derived from somatic mutations or intron retention is considered to be a risk factor for patient survival.[18,19] Clinical application of ICB for MM was not approved because most patients underwent relapse and had refractory features or serious adverse events.[20–22] The number of anti-myeloma cytotoxic T cells reinvigorated by ICB treatment is limited because myeloma-reactive T cells become impaired in progressive disease.[23] Moreover, T cells with exhaustion (PD-1, TIGIT,

Received 21 March 2023; accepted 12 May 2023;
https://doi.org/10.1016/j.omtm.2023.05.014.

Correspondence: Shin-ichiro Fujii, MD, PhD, Laboratory for Immunotherapy, RIKEN Center for Integrative Medical Sciences, 1-7-22, Suehiro-cho, Tsurumi-ku, Yokohama, Kanagawa 230-0045, Japan.
E-mail: shin-ichiro.fujii@riken.jp

CD160, and 2B4) or senescence (CD57) markers are frequently detected in the bone marrow of mice and patients with MM.[24,25] Although neoantigen-based therapy is attractive, augmentation with ICB treatment or vaccines may be insufficient to attain therapeutic effects in patients with progressed MM. Moreover, even detection of clinically relevant neoantigens is difficult in an autologous manner using patient-derived peripheral blood mononuclear cells (PBMCs). To overcome these obstacles, use of healthy donor (HD)-derived cytotoxic T lymphocytes (CTLs) against neoantigens has been proposed.[26] Especially when leveraged by third-party TCR repertoires that potentially recognize the broad spectrum of tumor neoantigens, application of neoantigen-specific TCR gene transfer will enable off-the-shelf but tailored immunotherapy. In fact, several studies using neoantigen-specific TCR-T cell therapy have demonstrated clinical responses.[27–30] Considering that TCR-T cell therapy targeting NY-ESO-1 has been reported to achieve high percentages of complete response (CR) and near-CR in patients with MM without adverse effects,[31] neoantigen-specific TCR-T cell therapy may achieve similar outcomes. Nevertheless, partly because of the scarcity of patient-derived xenograft models, except utilization of MM cell lines,[32] a proof of principle of HD-derived neoantigen-specific TCR gene application for treating MM has not been shown sufficiently, even in a preclinical model.

In the present study, we established a method to identify immunogenic mutant antigens on allogeneic tumor cells and a reactive TCR screen procedure using HD-derived PBMCs effectively. To demonstrate the MM-suppressive effect of the neoantigen-specific TCR gene *in vivo*, we aimed to detect immunogenic mutant antigens expressed in MM cells and to verify them in immunodeficient mice. After identifying mutant antigen candidates by immunogenomics analysis of MM cells, their immunogenicity was evaluated by examining the induction capability of CTLs. We successfully identified that HLA-A*24:02 restricted several immunogenic peptides and validated the corresponding TCR repertoires using single-cell TCR sequencing for peptide-reactive CTLs generated from HLA-A*24:02$^+$ HD-derived PBMCs. Particularly, the coenzyme A synthase (COASY) S55Y coding sequence was identified as an immunogenic epitope across several MM cells. The designated TCRs have reactivity and cytotoxicity against COASY S55Y on tumor cells in an HLA-A*24:02- and mutant gene-dependent manner. We also showed tumor suppression by adoptive cell transfer of mutant antigen-specific TCR-T cells in an MM cell-bearing xenograft model. The results showed the effectiveness and feasibility of HD-derived PBMCs to identify neoantigens and neoantigen-specific TCRs for prospective MM treatment.

RESULTS

Identification of neoantigen candidates and reactive TCR repertoires from HDs

We utilized publicly available RNA sequencing data from the Cancer Cell Line Encyclopedia (CCLE) to investigate potential neoantigens in MM.[33] After mapping, the SNPs and missense and insertion or deletion (indel) mutations were investigated by mutation caller. We used KMM-1, an HLA-A*24:02$^+$ MM cell line that was established from a subcutaneous plasmacytoma.[34] Because HLA-A*24:02 is the major allele in East Asia,[35,36] we focused on the HLA-A*24:02 allele in this study. All genes expressed with mutations were further parsed to select HLA-A*24:02 loadable peptides with predicted high affinity by NetMHCpan v.4.0[37] (Figure S1A). CD8$^+$ T cells from HLA-A*24:02$^+$ HDs were primed with 9-mer peptide-pulsed autologous dendritic cells (DCs) (pooled 2 to 3 peptides from 35 candidate peptides) (Table S1; Figure S1B). The CTL responses were monitored by activation markers (i.e., interferon [IFN]-γ production [ELISPOT assay] and CD137 upregulation [flow cytometry]) after stimulation with every single peptide (Figures S2A and S2B). The epitope-reactive CTL candidates were selected and expanded by an additional culture using the same single peptide-loaded DCs. Then, the cognate peptide-specific immune responses were investigated to confirm CTL induction and immunogenicity of their respective peptides (Figures 1A and S2B). We performed the screening from 7 HDs and detected 12 cumulative CTL lines against 7 peptides, which showed enhanced IFN-γ production by peptide stimuli (Figure 1B).

To identify the TCR repertoires from induced CTLs, the peptide-reactive CTLs were isolated using the CD107a degranulation assay. Subsequently, as described in Figure S1C, single-cell TCR sequencing was conducted (Figures 2A and S3A). TCRβ sequences were parsed by TCRdist[38] to assess the points of proportion and homology hierarchy in each HD (Figures 2B and S3B). Candidate TCRα and TCRβ repertoires were cloned from a major population of single CTL clones (Table S2). Their reactivity for KMM-1 or corresponding peptide-pulsed C1R-A*24:02 cells was investigated by transducing TCRs into SKW-3-hCD8AB cells, termed SKW-3-TCRs. Successful TCR expression was confirmed by CD3 membrane expression (Table S2). The reactivity was assessed by upregulation of CD69. Consequently, 3 TCRs for peptide 2 (QYSPVQATF, COASY S55Y), 6 TCRs for peptide 4 (IYLDLPWYL, TLR1 S602I), 1 TCR for peptide 5 (QYNKYVEVF, ZNF117 C83Y), and 1 TCR for peptide 23 (MYIEMLKSI, CENPBD1 T168I) were identified to possess peptide-specific responses and responses to KMM-1 (Figure S3C). Some SKW-3-TCRs highly expressed CD69 under basal conditions, suggesting that these TCRs probably possess tonic signals. Therefore, they were excluded from further analysis. The peptide-reactive TCRβ and TCRα were tandem linked with Furin-SGSG spacer-P2A sequences as in Figure S1C and further analyzed. The TCR IDs in this study were assigned as [HD number]-[peptide number]-[TCR number if assigned] (e.g., HD3-2-3, HD4-4). Tandem-linked TCR-expressed SKW-3-TCRs also conserved peptides and KMM-1 reactivity (Figure 2C). RNA sequencing of MM cells in CCLE were parsed to examine the mutations in these 4 genes and HLA-A type, as shown in Figure S4A. We also confirmed this mutated gene expression in KMM-1 by Sanger sequencing (Figure S4B).

Validation of COASY S55Y as a naturally processed epitope presented on HLA-A*24:02

The activation of SKW-3-TCRs by stimulation with titrated peptides was assessed to investigate mutation specificity. It revealed that all TCRs showed mutation-polarized reactivity (Figure 3). Compared

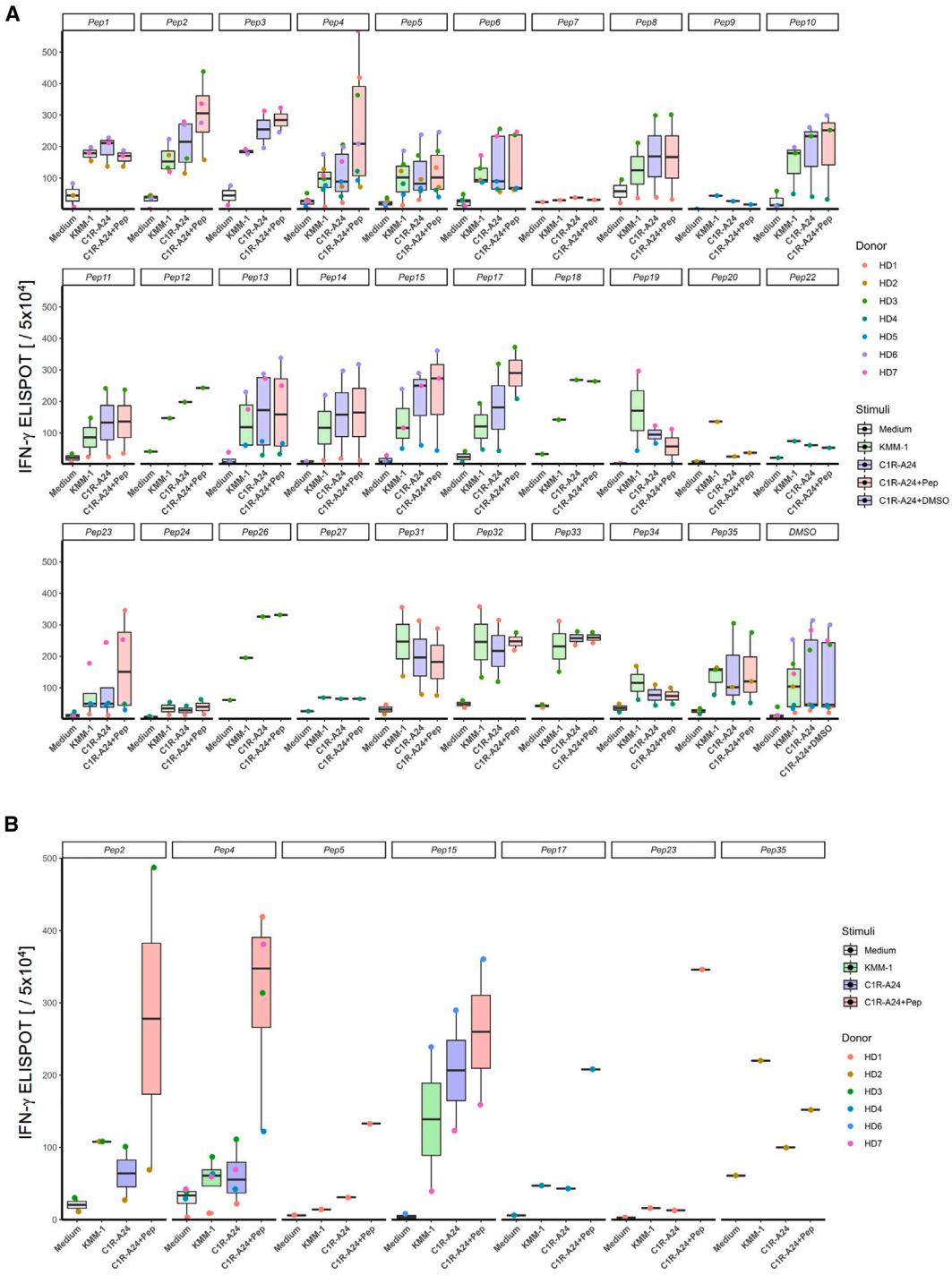

Figure 1. Screen of mutant antigen candidate peptides against MM

(A) Response of CTL lines against KMM-1 and mutant antigen candidates. To generate CTL lines, selected CTL candidates were cultured with single peptide-pulsed DCs for another one or two rounds. Expanded CTL candidates from different 7 donors were restimulated by KMM-1 or C1R-A*24:02 with the corresponding peptide for 20–24 h, and IFN-γ production was monitored. Boxplots represent the number of IFN-γ ELISPOTs. (B) Same as (A), but IFN-γ production from the mutant antigen peptide-specific CTLs from the different 6 donors is summarized.

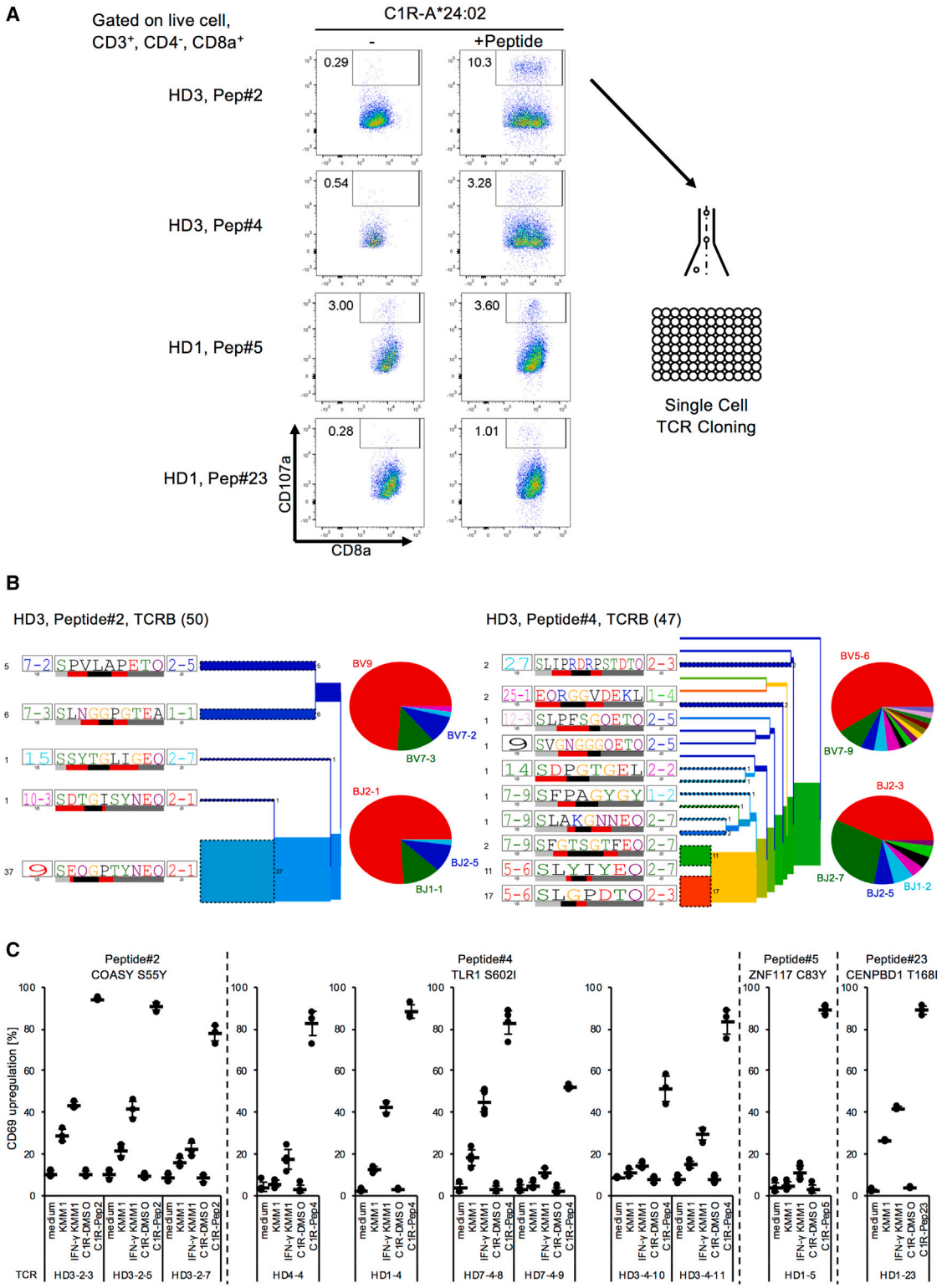

Figure 2. Evaluation of TCR repertoires for mutant antigen candidates

(A) Flow cytometry analysis of mutant antigen peptide-specific CTLs. Peptide-reactive CTLs were stimulated by C1R-A*24:02 pulsed with every single peptide with anti-CD107a antibody and GolgiStop for 3.5–4 h. CD107a-positive CD8+ T cells were sorted. (B) TCRdist analyses of TCRB repertoire sequences from sorted single cells. The tree

(legend continued on next page)

with neoantigens directly identified by liquid chromatography-tandem mass spectrometry (LC-MS/MS), neoantigen candidates listed by next generation sequencing (NGS) and affinity prediction algorithm occasionally contained immunogenic but not naturally processed epitopes.[39,40] To validate the TCR responses against naturally processed antigens, we isolated neoantigen candidate genes from KMM-1-derived cDNA and established the full length of mutant gene-overexpressing KMM-1 cells. Then, SKW-3-TCR reactivity for these mutant gene-transduced cells with or without stimulation by IFN-γ was analyzed. SKW-3-TCRs against COASY S55Y (HD3-2-3, HD3-2-5, and HD3-2-7) showed considerable responses to COASY S55Y-overexpressing KMM-1 cells. In contrast, no obvious augmented reactivity was observed in SKW-3-TCRs against TLR1 S602I (HD4-4, HD1-4, HD7-4-8, HD7-4-9, HD3-4-10, and HD3-4-11), ZNF117 C83Y (HD1-5), and CENPBD1 T168I (HD-1-23) for their respective mutant gene-overexpressing KMM-1 cells (Figure 4A). These results demonstrated that TCRs (HD3-2-3, HD3-2-5, and HD3-2-7) recognized the COASY S55Y peptide and that this epitope is naturally presented on the tumor surface regardless of IFN-γ priming. To confirm that SKW-3-TCRs (HD3-2-3, HD3-2-5, and HD3-2-7) show mutation-specific response in an HLA-A*24:02-restricted manner, we investigated the activation of SKW-3-TCRs by coculture with the COASY S55Y gene and cognate COASY wild-type (WT) gene-overexpressing C1R-A*24:02 cells. The SKW-3-TCRs only reacted with COASY S55Y gene-overexpressing C1R-A*24:02 cells but not COASY WT gene-overexpressing C1R-A*24:02 cells (Figure 4B). Thus, we revealed the immunogenicity of COASY S55Y (QYSPVQATF) mutation on HLA-A*24:02 as a mutant antigen and successfully isolated the corresponding TCR sequences.

Neoantigens are amino acid peptides derived from somatic mutation with HLA restriction. To verify that COASY S55Y mutation is widely used as a common mutant antigen, we examined whether these TCRs respond solely to target cells with a gene mutation depending on HLA types across tumors. First, we investigated whether the SKW-3-TCRs (HD3-2-3, HD3-2-5, and HD3-2-7) showed specific activation against other MM cells in the COASY S55Y mutation and HLA-A*24:02 manner. To select the target MM cells, referring to the NGS analysis result shown in Figure S4A, we confirmed by Sanger sequencing and flow cytometry analysis that KMM-1, KMS-11, and KMS-21BM are COASY S55Y^{+}HLA-A*24:02^{+} cells, RPMI-8226 and KMS-12-BM are COASY S55Y^{+}HLA-A24*02^{-} cells, and KMS-28 is a COASY S55Y^{-}HLA-A*24:02^{+} cell (Figure S4C). When we cocultured SKW-3-TCRs (HD3-2-3, HD3-2-5, and HD3-2-7) with them, we found that all SKW-3-TCRs recognized COASY S55Y^{+}HLA-A*24:02^{+} MM cells (KMM-1, KMS-11, and KMS-21BM). However, they did not respond against COASY S55Y^{+}HLA-A24*02^{-} and COASY S55Y^{-}HLA-A*24:02^{+} cells, except that SKW-3-TCR (HD3-2-5) also reacted with COASY S55Y^{-}HLA-A*24:02^{+} MM cells (Figure 4C). Next, we examined whether the TCRs can recognize the mutation on other types of tumors. Because we confirmed that 888-mel cells (melanoma) express COASY S55Y, we observed the specific response against 888-mel but not SW480 (colon cancer) and PC-3 (prostate cancer) cells (Figures S5A and S5B). We concluded that these TCRs have a determinate capacity to recognize mutation gene expression with HLA restriction irrespective of cell type.

SKW-3-TCRs (HD3-2-3 and HD3-2-5) showed high reactivity, while SKW-3-TCRs (HD3-2-7) showed less. To discuss this variation, we applied the amino acid sequences of these TCRs for different TCR/major histocompatibility complex (MHC)/peptide modelers[41–43] to understand the 3D structure models and focused on their interaction. The binding affinity between modeled TCRα/TCRβ and the MHC class I/peptide complex was calculated by PRODIGY, which can predict protein-protein complex interaction based on atomic coordinates.[44] The predicted ΔG energy indicated a more stabilized interaction of HD3-2-3, HD3-2-5, and HLA-A*24:02/QYSPVQATF than that of HD3-2-7, which coincided with the biological results. Furthermore, the predicted affinity is comparable with a previous report that showed the high-affinity interaction observed in TCRs and the HLA-A*24:02/Nef (peptide from HIV-1) complex, whose crystal structures were registered in the Protein Data Bank (Figure S6A). Indeed, spatial analysis in the 3D-modeled structures clarified the potential interaction (hydrophobic interaction and hydrogen bond) between QYSPVQATF and TCRβ CDR3 regions of HD3-2-3 and HD3-2-5. It may possibly suggest the attribution of complex stability (Figure S6B). Although further studies are needed, these observations would be helpful to show that there are neoantigen-reactive TCRs with high affinity in HDs.

Immunological evaluation of COASY S55Y-specific TCR-T cells against tumor cells

To investigate whether HLA-A*24:02/COASY S55Y-specific TCRs effectively show cytotoxicity against MM cells, a functional assay of TCR-T cells was conducted, using PBMCs from several HLA-A*24:02^{+} HDs. To enhance the expression efficiency of exogenous TCRs and to distinguish them from endogenous TCRs, each constant region was replaced by mouse constant regions.[45] After showing that the original TCR transduction conferred T cell reactivity against COASY S55Y peptide-pulsed C1R-A*24:02, we also confirmed that the murinization (HD3-2-m3, HD3-2-m5, and HD3-2-m7) facilitates T cell activation in each TCR in this study (Figure 5A). Henceforth, murinized TCRs were transduced into PBMCs from HDs. After expansion and purification, we obtained sufficient numbers of HLA-A*24:02/COASY S55Y-specific TCR-T cells that were verified by dextramer and mouse TCRβ antibody staining (Figure 5B). Then, we investigated the cytolytic activity of TCR-T cells against

diagrams show CDR3 hierarchy and VDJ proportion. The pie charts summarize the TRBV and TRBJ proportion. The numbers in parentheses indicate the parsed single clones. (C) Evaluation of the reconstituted TCR responses against KMM-1 and mutant antigen candidates. SKW3-hCD8AB cells were transduced with tandem-linked TCR vectors and cocultured with KMM-1, IFN-γ activated KMM-1, C1R-A*24:02, or the corresponding peptide-pulsed C1R-A*24:02 for 18–24 h. Then, CD69 upregulation of CD8B^{+}GFP^{+} cells was analyzed using flow cytometry. The percentages of CD69 were plotted. Data were pooled from three or four independent experiments. The values show mean ± SD.

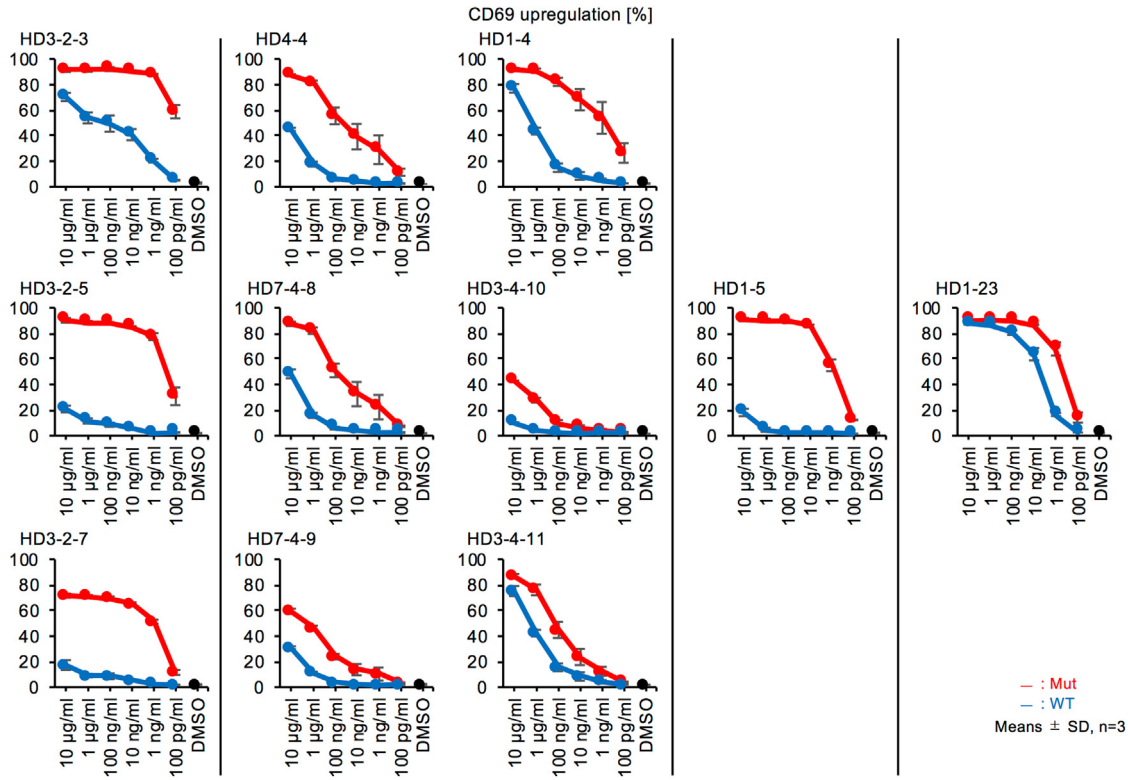

Figure 3. Peptide titration of mutant antigen-specific TCRs

SKW3-hCD8AB cells transduced with the indicated TCR were cocultured with C1R-A*24:02 cells in the presence of titrated mutant (red) or counterpart (blue) peptides for 18–24 h. CD69 upregulation in $CD8B^{+}GFP^{+}$ cells was assessed by flow cytometry. The percentages of CD69 were plotted. Data were pooled from three independent experiments. The values show mean ± SD.

peptide-pulsed C1R-A*24:02 cells. All TCR-T cells showed cytotoxicity against mutation-specific targets with high sensitivity, reaching a 100 pg/mL order, as low as naturally detected peptide amounts in tumors, particularly in the HD3-2-m3 (Figure 5C). Furthermore, by titration, HD3-2-m3 and HD3-2-m5 showed higher affinity than HD3-2-m7, similar to previous results. Next, we examined the tumoricidal activity against endogenously expressed tumor antigens in MM cells. When HLA-A*24:02^{+} COASY S55Y^{+} MM cells (i.e., KMM-1, KMS-11, and KMS-21BM), were used as target cells, TCR-T cells decorated with HD3-2-m3 and HD3-2-m5 showed significantly enhanced tumoricidal activity, but not against autologous PHA-blasts (Figure 5D). Thus, these TCR repertoires conferred tumor-killing activity to T cells from all HLA-A*24:02^{+} HDs. Furthermore, we selected HD3-2-m3 as the most functional TCR in terms of sensitivity and specificity, and it was further subjected to *in vivo* analysis.

Therapeutic application of HLA-A*24:02/COASY S55Y-specific TCR-T cells against MM cells

We conducted *in vivo* studies by adoptive transfer of TCR (HD3-2-m3)-T cells to MM-bearing mouse models. We established Akaluc-expressing KMS-11 MM cells to monitor the tumor burden after intravenous injection of TCR-T cells; a detailed experimental schematic is shown in Figure 6A. We observed significant tumor regression in TCR-T cell-treated mice compared with mock transduced T cell-treated mice (Figures 6B and 6C) and prolonged survival (Figure 6D) (median survival of 79.5 days in the non-treated group, 87 days in the mock T cell-treated group, and 99.5 days in the TCR [HD3-2-m3]-T cell-treated groups).

To examine the probability of this mutant epitope for MM patients, we investigated the RNA sequencing of MM cells from several reports. Although we could not analyze each patient-matched non-tumor tissue, there are possible compatibilities of this target epitope (Figure S7).

Overall, we initially showed that COASY S55Y-targeting TCR-T cells exert anti-myeloma activity in a mouse model. Our study suggested that neoantigen-specific TCR genes discovered in HDs will serve as a potential therapeutic resource for treating patients with MM the same as other tumors in the future, and our proposed strategy can contribute to its development in a cost-effective and timely manner (Figure 7).

DISCUSSION

Adoptive cell transfer of tumor-targeting T cells (TILs, CAR-T cells, and TCR-T cells) showed drastic clinical responses.[46] Because of this, it is important to utilize tumor-specific targets. Hence, application of TCR-T cell therapy for neoantigens, in addition to conventional

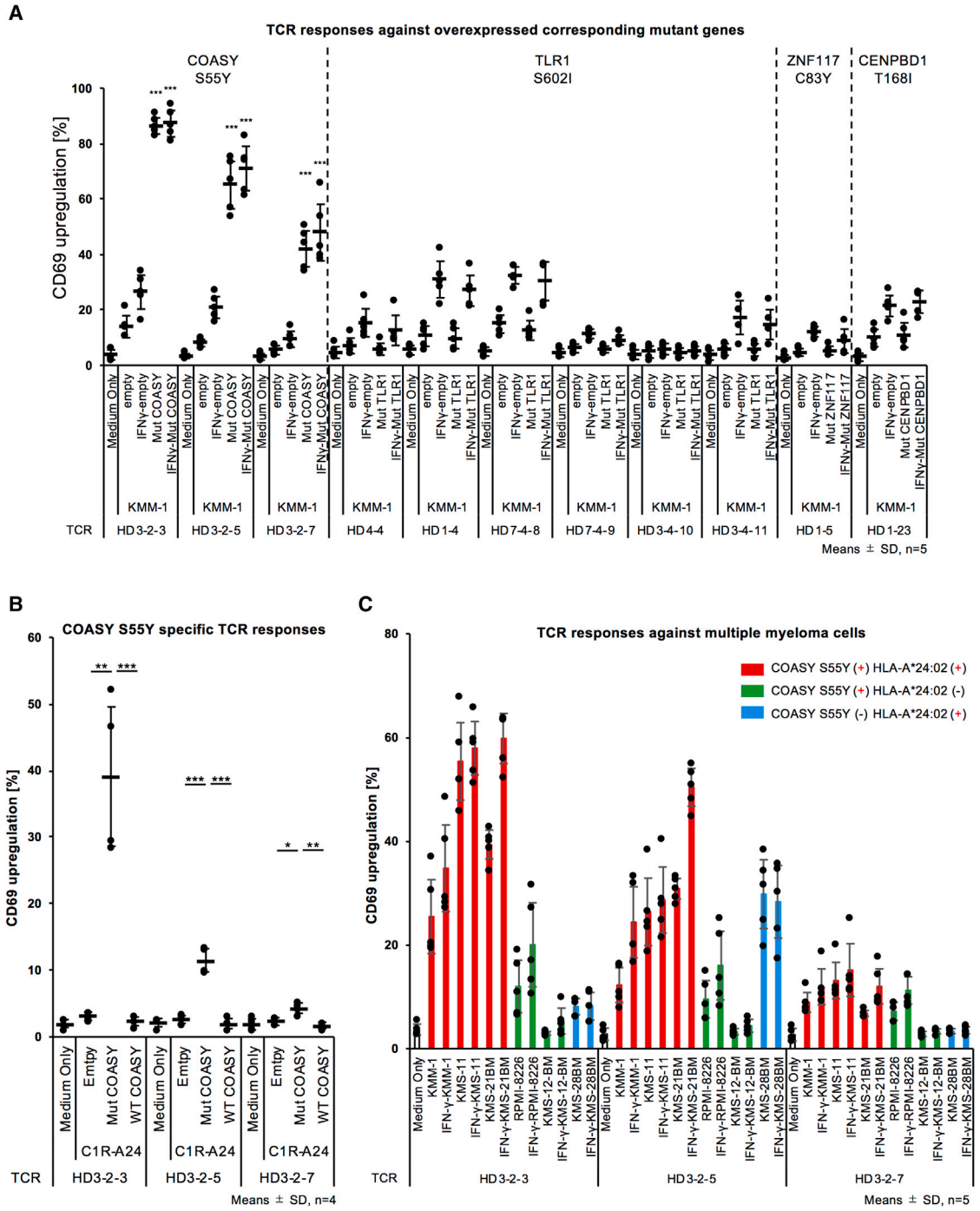

Figure 4. COASY S55Y restricted on HLA-A*24:02 as common antigens in MM

(A) Four mutant antigen candidate genes were transduced into KMM-1 cells. SKW3-hCD8AB cells transduced with relevant TCRs were cocultured with IFN-γ unprimed/primed mutant gene-expressing KMM-1 cells for 18–24 h. CD69 upregulation in $CD8B^{+}GFP^{+}$ cells was analyzed using flow cytometry. The percentages of CD69 were plotted. Data were pooled from five independent experiments. The values show means ± SD. (B) COASY S55Y and COASY S55S were overexpressed in C1R-A*24:02 cells. SKW3-hCD8AB cells transduced with COASY S55Y-specific TCRs were cocultured with C1R-A*24:02 cells for 18–24 h. CD69 upregulation in $CD8B^{+}GFP^{+}$ cells was analyzed using flow cytometry. The percentages of CD69 were plotted. Data were pooled from four independent experiments. The values show means ± SD. (C) Mutant antigen-specific responses across MM cells. SKW3-hCD8AB cells transduced with COASY S55Y-specific TCRs were cocultured with six MM cell lines in the presence or absence of IFN-γ priming for 18–24 h. CD69 upregulation in $CD8B^{+}GFP^{+}$ cells was analyzed using flow cytometry. The percentages of CD69 were plotted (red, COASY $S55Y^{+}$HLA-A*24:02^{+}; green, COASY $S55Y^{+}$HLA-A*24:02^{-}; blue, COASY $S55Y^{-}$HLA*A24:02^{+}). Data were pooled from five independent experiments. The values show means ± SD.

(legend continued on next page)

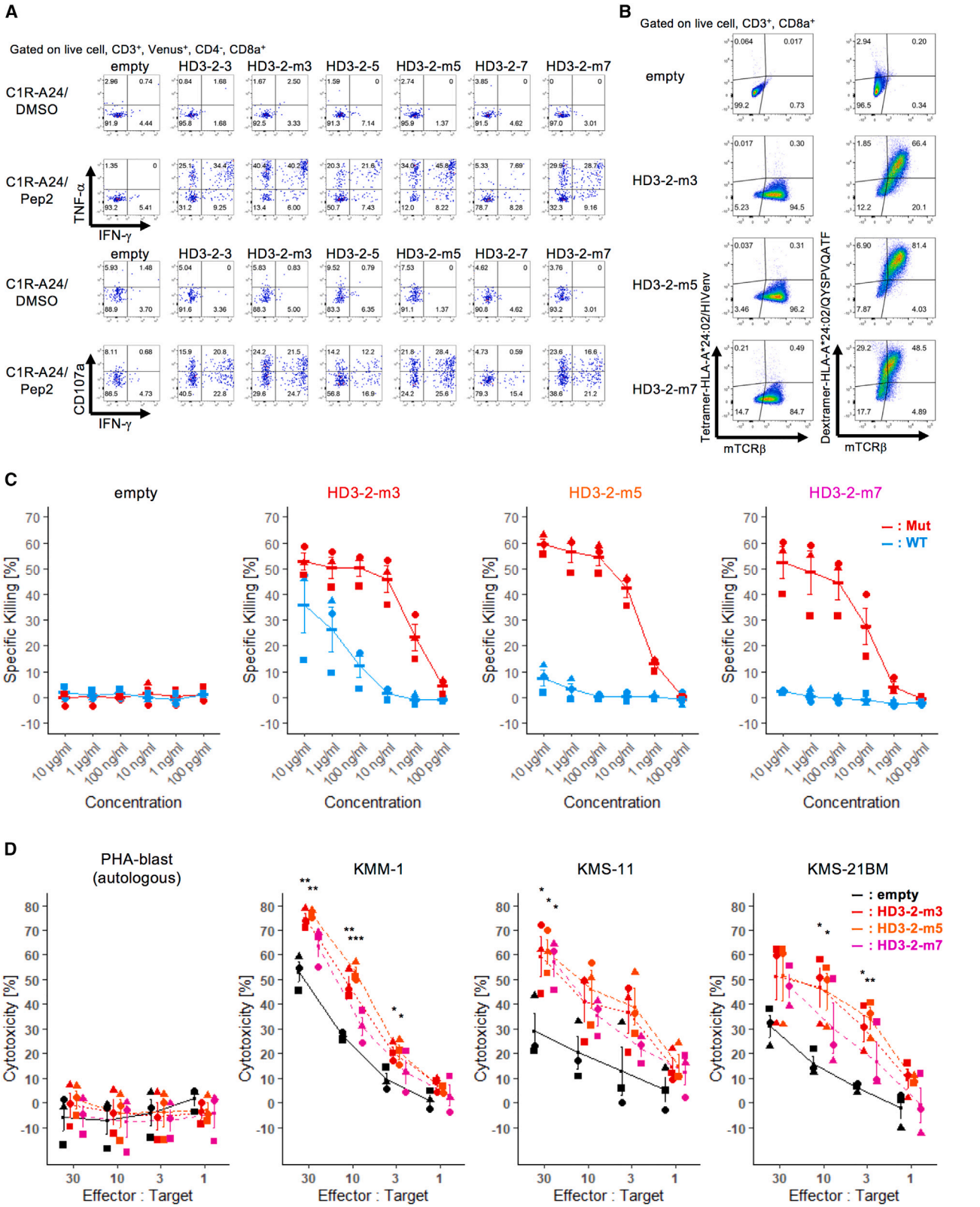

(legend on next page)

tumor-associated antigens or oncovirus antigens,[47,48] should be examined for clinical efficacy and feasibility. In this study, we established a series of screening procedures that effectively identify tumor-derived mutant antigens and their corresponding TCR repertoires from HDs. We used immunogenomics and immunobiological approaches with single-cell TCR sequencing. Consequently, we successfully identified an immunogenic mutant antigen peptide, COASY S55Y, and verified that HLA-A*24:02/COASY S55Y-specific TCRs recognized several MM cells as a shared antigen. Furthermore, reconstituted TCR-T cells showed tumor-lytic activity. Finally, when we used MM cells expressing endogenous antigen in the *in vivo* model, we found that adoptive cell transfer of COASY S55Y-specific TCR-T cells showed an antitumor effect. Collectively, we demonstrated COASY S55Y to be an experimental neoantigen candidate across several tumors and showed potential therapeutic application of tumor-derived mutant antigen-specific TCR genes from HDs to suppress MM.

This study aimed to identify neoantigen candidates from tumor mutations in allogeneic tumors for individual neoantigen therapy as personalized medicine. This has pros and cons, and caution should be exercised. There is a sufficient advantage in identifying neoantigens from a small amount of tumor cells for genomics analyses and HD-derived peripheral blood without using a large amount of patient-derived peripheral blood. The use of HD samples overcome a scarcity of tumor-reactive T cells in patients with progressed malignancy because of immune dysfunction and hematopoietic abnormality. Additionally, to the best of our knowledge, no study has proven the utility of HD-derived mutant antigen-specific TCR genes for suppressing MM in mouse models. Our results suggest that targeting neoantigens is worth investigating for future treatment of patients with MM, and our system is also useful for detecting neoantigens and specific TCRs. With recent advances in mutation calling, even without matched normal tissues,[49,50] targeting neoantigens will be widely used in clinical settings. In contrast, allogeneic TCRs comprise a risk factor for cross-reactivity to unexpected miscellaneous antigens in recipients. Despite the previous success of TCR-T cell therapy, adequate caution is invariably required, particularly when individual immune responses are observed.

Neoantigen-based immunotherapy is an intriguing therapeutic approach; however, identifying clinically relevant neoantigens requires more effort. Infallible selection from neoantigen candidates revealed by immunogenomics and immunopeptidomics requires experimental validation. Hence, it may not be useful for urgent application against rapidly growing tumors. On the contrary, MM is a good target because its progression is slower, taking a long time to progress after diagnosis at an early stage. The process from asymptomatic premalignant status (i.e., monoclonal gammopathy of undetermined significance [MGUS] and smoldering MM [SMM]) to onset usually takes a long time. This may be mechanistically due to hyperdiploidy (trisomy of odd-numbered chromosomes) or chromosomal translocation (IGH loci at chromosome 14q and driver genes such as CCND1 (t[11;14]), FGFR3 (t[4;14]), and c-Maf (t[14;16]) preceding onset. After therapeutic intervention, additional genomic abnormalities, such as copy number alteration (17p deletion, 1q amplification), oncogenic mutations (NRAS, TP53, TET2, TRAF2, NF1, and ARID2), and increased AID/APOBEC activity multilaterally give rise to drug resistance or relapse of MM.[51,52] Additionally, the clonal evolution of MM cells leads to the heterogeneity of tumor cells in intra- (regionally) and inter-patients.[53,54] Despite variational evolution, a comparative study analyzing the transition from MGUS/SMM to MM revealed that the heterogeneity and clonality of tumor cells were stabilized under progression[55] and that additional mutations cumulatively increased.[17] Regarding the immunological aspect, tumor-reactive stem-like/tissue-resident T cells were enriched in the bone marrow of patients with MGUS but decreased in that of patients with MM.[56] Therefore, clinical application targeting neoantigens would be suitable for the early stage of MM with slower-progressing tumors.[57] Subsequently, these strategies would be useful if multiple sets of the shared neoantigens were built up and corresponding TCRs were identified.

Finally, this study demonstrated that COASY S55Y-TCR responds to MM and melanoma cells. When neoantigens based on genetic analysis are identified, the tumor-lytic activity against other tumor types can be examined. This does not preclude the considerable effort needed. Here, our approach may fulfill the demand for identifying the pairs of patients' neoantigens and their corresponding TCRs in HDs. With a strategy of enhancing infused T cells,[58,59] neoantigen-specific TCR-T cell therapy will achieve unprecedented clinical outcomes in the future.

MATERIALS AND METHODS

Cell culture

SKW-3 was provided by the RIKEN BioResource Research Center (RCB1168). To generate SKW-3-hCD8AB cells, pMXs-hCD8A-IRES-Puro and pMXs-hCD8B-IRES-Puro were retrovirally transferred into SKW-3, and $CD8a^{+}CD8b^{+}$ cells were regularly sorted and maintained using 3 μg/mL puromycin. C1R-A*24:02 cells, lymphoblastoid C1R

Figure 5. Cytolytic function of COASY S55Y-specific TCR-T cells against MM cells

(A) COASY S55Y-specific TCR were transduced to donor PBMCs. TCR-T cells were sorted using a fluorescence marker. After coculturing with peptide-pulsed C1R-A*24:02 cells in the presence of anti-CD107a antibody, brefeldin A, and monensin for 16 h, IFN-γ and TNF-α production in $CD8^{+}$ T cells was analyzed. "m" means murinization of the constant region of TCRs. (B) COASY S55Y-specific mTCRs were transduced to donor PBMCs. Three TCR-T cells were enriched by biotin anti-mouse TCRβ antibody labeling, followed by MACS. COASY S55Y-specific TCR-T cells were verified using dextramer-HLA-A*24:02/QYSPVQATF and anti-mTCRβ antibodies. The HLA-A*24:02/HIVenv tetramer was used as a negative control stain. (C) Mutant antigen peptide-specific cytotoxicity of TCR-T cells. TCR-T cells were cocultured with C1R-A*24:02 cells pulsed by titrated mutant or counterpart peptide as target cells for 18–24 h. Data were pooled from three independent donor experiments, and the values show mean ± SEM. Different dots indicate each donor. (D) Cytotoxicity against HLA-A*24:02^{+} COASY $S55Y^{+}$ MM cells of TCR-T cells. TCR-T cells were cocultured with MM cells or cognate-donor derived PHA-blasts as target cells for 18–24 h. Data were pooled from three independent donor experiments, and the values show mean ± SEM. Different dots indicate each donor.

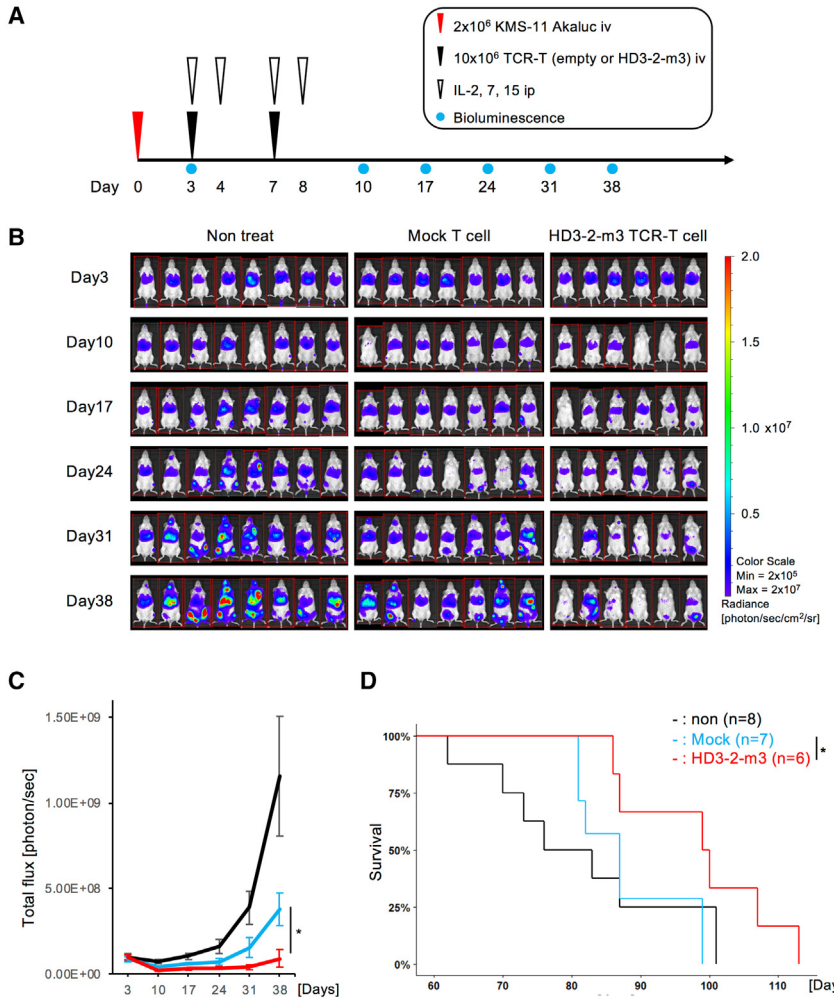

Figure 6. Antitumor effect of COASY S55Y-specific TCR-T cell treatment in a tumor-bearing xenograft model

(A) Experimental scheme of xenograft models. KMS-11-Akaluc-TdTomato cells (2×10^6 cells/mouse) were intravenously injected into female NOG mice. Three days later, tumor-derive bioluminescence was measured to confirm tumor engraftment and randomize. Mice were divided into three groups: non-treated, mock-transduced T cell-treated, and HD3-2-m3-transduced T cell-treated. Mock-transduced T cells or HD3-2-m3 TCR-T cells (10×10^6 cells/mouse) were intravenously injected on days 3 and 7. IL-2, IL-7, and IL-15 cocktails were intraperitoneally injected on days 3, 4, 7, and 8 in the T cell treatment group. Tumor-derived bioluminescence for three mouse groups was measured on the indicated days. (B) Bioluminescence images showing tumor burden in all mice on the indicated days. (C) Measurement of tumor growth. The x axis indicates days after administration of KMS-11-Akaluc-TdTomato cells, and the y axis indicates bioluminescence. The values show mean ± SEM. (D) Survival analysis of each group: non-treated (black, n = 8), mock-transduced T cell-treated (blue, n = 7), and HD3-2-m3 TCR-transduced T cell-treated (red, n = 6). Data were pooled from three independent experiments.

cells which lack HLA-A and -B expression, transfected with HLA-A*24:02 were provided by Dr. M. Takiguchi (Kumamoto University School of Medicine, Japan) and maintained using 100–200 μg/mL Hygromycin B Gold (Invivogen). KMM-1, KMS-21BM, and KMS-12-BM were provided by Dr. Hata (Kumamoto University School of Medicine, Japan). KMS-11 and RPMI-8226 were provided by Dr. Yasukawa (Ehime University, Japan). KMS-28BM was purchased from the JCRB Cell Bank (JCRB1192). KMM-1 cells retrovirally transduced with neoantigen-IRES-Puro were selected using 2–3 μg/mL puromycin. All blood cell lineage cells and assay conditions were maintained using RPMI-1640 medium supplemented with 10% fetal bovine serum (FBS), 55 μM 2-ME, and 1% 5,000 U/mL penicillin/5,000 μg/mL streptomycin solution (Gibco). SW480 and PC3 were purchased from the ATCC (CCL-228 and CRL-1435, respectively) and maintained in RPMI-1640 medium supplemented with 10% FBS and 1% penicillin/streptomycin solution. Plat GP was provided by Dr. Kitamura (Tokyo University, Japan) and maintained using 10 μg/mL blasticidin. HEK293T cells were purchased from the RIKEN BRC (RCB2202) and maintained using 500 μg/mL G418. 888-mel was a kind gift from Dr. S.A. Rosenberg (NIH, USA) and was maintained in DMEM (high glucose) supplemented with 10% FBS and 1% 5,000 U/mL penicillin/5,000 μg/mL streptomycin solution.

Reagents

pMXs-IRES-GFP was purchased from Cell Biolabs (San Diego, CA, USA). pMSCV-IRES-GFP was a kind gift from Dario Vignali (Addgene plasmid 52107). pBApo-EF1a Pur was purchased from Takara Bio (Shiga, Japan). CSII-EF-MCS, CSII-EF-MCS-IRES2-Venus, pCAG-HIVgp, and pCMV-VSV-G-RSV-Rev, kind gifts from Dr. H. Miyoshi, were provided by the RIKEN BRC through the National BioResource Project of the MEXT/AMED, Japan (RDB04378, RDB04384, RDB04394, and RDB04393, respectively).

Human samples and preparation

Human peripheral blood was obtained from HDs in the RIKEN Center for Integrative Medical Sciences. PBMCs were prepared from fresh whole blood by Ficoll-Paque Plus (Cytiva, Tokyo, Japan) density gradient centrifugation. PBMCs were washed twice with phosphate-buffered saline (PBS) and cryopreserved. HLA-A2 and A24 expression was examined by antibody staining followed by flow cytometry analysis. COASY S55Y SNP was investigated by Sanger sequencing of PCR-amplified cDNA derived from PBMCs. HD information is shown in Table S3. The RIKEN institutional review board approved all studies.

CTLs induction against neoantigens candidate peptides

$CD8^+$ or $CD14^+$ cells were enriched by human CD8 or CD14 MicroBeads (Miltenyi Biotec), respectively. $CD14^+$ cells were cultured

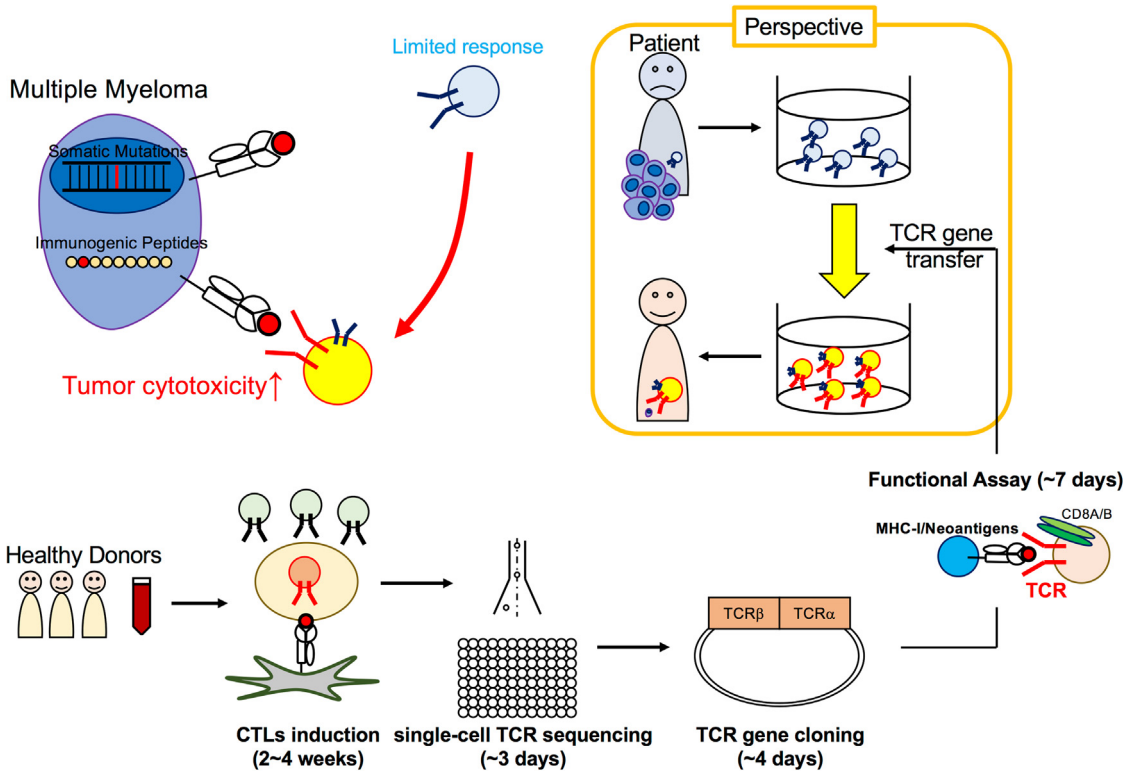

Figure 7. Research summary

A mutant antigen-specific TCR sequence was detected in HD-derived PBMCs through CTL induction, single-cell TCR sequencing, and cloning, followed by a functional assay. The mutant antigen-specific TCR gene transfer conferred anti-myeloma activity. The system will be scalable for further identification of clinically relevant neoantigens.

with 100 ng/mL GM-CSF (R&D Systems) and 25 ng/mL interleukin-4 (IL-4) (R&D systems) for 6 days to differentiate into DCs. On day 5, 10 ng/mL IL-6 (R&D Systems), 10 ng/mL IL-1β (R&D Systems), 10 ng/mL tumor necrosis factor alpha (TNF-α) (R&D Systems), and 1 μg/mL PGE2 (Sigma-Aldrich, P5640, Tokyo, Japan) were added for DC maturation. All cells were cryopreserved unless they were required for immediate use. For the first round of stimulation, 5×10^5 $CD8^+$ cells were cocultured with 5×10^4 DCs in the presence of pooled peptides (3.3 μg/mL each peptide) for 12 days. 100 U/mL IL-2 (Shionogi), 5 ng/mL IL-7 (PeproTech, Cranbury, NJ, USA), and 5 ng/mL IL-15 (PeproTech) were added from day 3. For the second round, proliferated cells were restimulated with a 10–50:1 ratio of DCs. Cytokine-containing fresh medium was periodically added every 2 or 3 days. For the third or fourth round, peptide reactive cells were further cocultured with a 5–50:1 ratio of DCs with a 3 μg/mL single peptide. Responses to corresponding single peptides were monitored by IFN-γ ELISPOT assay or CD137 upregulation by fluorescence-activated cell sorting (FACS) 20–24 h after C1R-A*24:02 and 10 μg/mL peptide stimulation.

ELISPOT assays

ELISPOT assays for antigen-specific IFN-γ secreting cells (BD Biosciences) were performed on 96-well filtration plates (MultiScreenHTS HA Filter Plate, 0.45 μm, clear, sterile) coated with 5 μg/mL Purified NA/LE Anti-Human IFN-γ in PBS. 5×10^4 CTLs stimulated by 1×10^4 C1R-A*24:02 cells in the presence or absence of 10 μg/mL peptides or 1×10^4 KMM-1 cells for 20–24 h.

Flow cytometry analysis

For cytokine staining, 5×10^4 T cells were cocultured with 5×10^4 peptide-pulsed C1R-A24 cells in the presence of 1.25 μg/mL anti-CD107a antibody, 1,500× GolgiSTOP, and 1,000× GolgiPlug for 16 h. Surface staining was followed by fixation, and cytokines were stained. BD Cytofix/Cytoperm and eBioscience permeabilization buffer were used for fixation and permeabilization, respectively. For dextramer staining, 2×10^5 cells were blocked by Human TruStain FcX (BioLegend, 422301). Subsequently, a custom dextramer for HLA-A*24:02/QYSPVQATF (Immudex, Virum, Denmark) or T-Select HLA-A*24:02 negative (HIV env) tetramer-RYLRDQQLL-PE (MBL, Tokyo, Japan) were added to stain for 15 min at room temperature, followed by surface antibody staining at 4°C. The Live/Dead Fixable Aqua Dead Cell Stain Kit, at 405 nm excitation (Thermo Fisher Scientific, Tokyo, Japan) was used to remove dead cells. The antibodies are listed in Table S4. Data were acquired by FACS Canto 2 and analyzed using FlowJo.

Single-cell TCR sequencing and construction of retroviral TCR vectors

Single-cell TCR sequencing was performed as referred to in our previous study[35] with modifications. All primers are listed in Table S5.

Neoantigen peptide-specific CTLs were stimulated with 10 μg/mL peptides in the presence of 1.25 μg/mL anti-CD107a antibody and 1,500× GolgiSTOP (monensin) for 3.5–4.5 h and then stained with anti-CD3, CD4, CD8a, and aqua. Using the FACSAria 3 cell sorter, peptide-specific cells gated on $CD3^+CD4^-CD8a^+CD107a^+$ cells were single cell sorted into 5 μL of RT-PCR mix on 96-well plates. The RT-PCR mix was composed of 1 μL of 5× Prime STAR GXL buffer, 0.45 μL of RT-PCR primer mix, 0.4 μL of 2.5 mM dNTP, 0.05 μL of 40 U/μL RNase inhibitor, 0.1 μL of 200 U/μL PrimeScript II reverse transcriptase (Takara Bio, Shiga, Japan), 0.05 μL of 1.25 U/μL PrimeSTAR GXL DNA polymerase (Takara Bio), and 2.95 μL of nuclease-free water. The program for the one-step RT-PCR was as follows: 45°C for 40 min, 98°C for 1 min and 35 cycles of 98°C for 10 s, 55°C for 15 s, and 68°C for 1 min. The resultant one-step RT-PCR products were diluted 10-fold with nuclease-free water and used as templates for the second PCR reaction. The second PCR reaction was performed using PrimeSTAR GXL with the pMXs-BamHI-InFusion primer and CA-rev2 primer for TCRa or CB-rev2 primer for TCRb in a total volume of 10 μL. The program for the second PCR was as follows: 98°C for 1 min and 44 cycles of 98°C for 10 s, 55°C for 15 s, and 68°C for 1 min. After ExoSAP-IT PCR Product Cleanup Reagent (Thermo Fisher Scientific, Tokyo, Japan) treatment, the second PCR products were directly sequenced using the CA-rev3 primer for TCRa or the CB-rev3 primer for TCRb at Eurofins Genomics (Tokyo, Japan). Sequencing results were analyzed using TCRdist[38] and the V-QUEST tool of the IMGT database (http://www.imgt.org/IMGT_vquest/input).[60] For TCR expression vector cloning, VDJ and C regions were amplified from the second PCR reaction products and donor PBMC-derived cDNAs, respectively. PrimeSTAR Max was used for amplification with the pMXs-BamHI-InFusion primer and CA-rev3 or CB-rev3 primer. Each fragment was recombined into BamHI-digested, linearized pMXs-IRES-GFP for TCRA or TdTomato for TCRB by InFusion HD reaction. Peptide-reactive TCRB and TCRA were linked with the Furin-SGSG-P2A spacer into pMXs-IRES-GFP by InFusion HD reaction. For expression in PBMCs, TCRB-P2A-TCRA sequences were recombined into CSII-EF-MCS or CSII-EF-MCS-IRES2-Venus by InFusion HD reaction. To facilitate expression, TCR constant regions were replaced by mouse origin (TRBC2 and TRAC). Each VDJ sequence can be found in Table S6.

Retrovirus or lentivirus transduction

pMXs or pMSCV vectors and VSV-G were co-transfected with a 3:1 ratio into Plat-GP cells using FuGene6 (Promega) or PEI-MAX (molecular weight [MW] 40,000) (Cosmo Bio, Tokyo, Japan), followed by a medium change. CSII-EF-MCS or CSII-EF-MCS-IRES2-Venus vectors, pCAG-HIVgp, and pCMV-VSV-G-RSV-Rev were co-transfected with a 2:1:1 ratio into HEK293T cells using PEI-MAX (MW 40,000), followed by a medium change. The virus-containing medium was harvested at 48 h (or an additional 24 h) after the medium change. Lentiviruses were concentrated by overnight centrifugation (8,000 × *g*) after filtration for transduction to PBMCs. The retrovirus or lentivirus was transduced into target cells in the presence of 5 μg/mL Polybrene (Nacalai) by plate centrifugation at 2,300 rpm for 99 min at 35°C.

Electroporation

Approximately 8 μg of pBApo-EF1a-emtpy/Mut COASY/WT COASY-SV40-Puro plasmid and at least 5×10^6 C1R-A*24:02 cells were electroporated at 500 V, 3 ms. Approximately 24 h thereafter, electroporated cells were selected using 2–3 μg/mL puromycin for an additional 48-h culture. Dead cells were removed by Ficoll gradient centrifugation.

CD69 upregulation assay

TCRs-coding retrovirus were transduced into SKW-3-hCD8AB cells in the presence of 5 μg/mL Polybrene (Nacalai) by centrifugation at 2,300 rpm for 99 min at 35°C. TCR expression was determined by CD3 cell surface expression. Unsorted TCR-transduced SKW-3-hCD8AB cells were cocultured with the target cells for 20–24 h in 96-well round-bottom plates. Target cells were pretreated using 10 ng/mL IFN-γ for 48 h where indicated. Approximately 5×10^4 SKW-3 cells were stimulated by $1-2 \times 10^4$ KMM1 cells, $1-2 \times 10^4$ neoantigen gene-transduced KMM1 cells, 1×10^4 C1R-A*24:02 cells with or without the indicated peptides, 3×10^4 neoantigen gene-electroporated C1R-A*24:02 cells, and 2×10^4 SW480, PC3, and 888-mel cells. The percentage of CD69 upregulation in gated-on live cells, $CD8b^+$, $GFP^+TdTomato^+$, or GFP^+ cells was assessed by FACSCanto II.

Pipelines identifying neoantigen candidate peptides

RNA sequencing (RNA-seq) data were downloaded using the SRAtoolkit fasterq-dump command. FASTQ data were mapped onto the human reference genome (GRCh38) by STAR with two-pass alignment mode.[61] The bam files were processed to remove PCR duplicates (Picard), inaccurate spliced reads, and indel realignment, followed by base recalibration referring to SNP vcf files (Homo_sapiens_assembly38.dbsnp138., Homo_sapiens_assembly38.known_indels., Mills_and_1000G_gold_standard.indels.hg38., and 1000G_phase1.snps.high_confidence.hg38.). Variants were called using GATK HaplotypeCaller[62] and mpileup (Samtools), followed by VarScan 2.[63] Common mutation sites extracted by bcftools were annotated by ANNOVAR. The amino acid sequences surrounding missense or indel mutation sites were listed by Isovar. Concomitantly, HLA typing was performed by using arcasHLA.[64] The neoantigen candidate sequences in KMM1 restricted on the HLA-A*24:02 allele (9-mer) were selected by NetMHCPan v.4.0 in BA and EL mode.[37] The 35 peptides are [EL score > 0.8 and IC50 <50] or [IC50 < 100 and Mut IC50 < Cognate WT IC50]. The synthesized 9-mer peptides (purity > 90%) were purchased from ABclonal Biotechnology and dissolved in DMSO.

3D modeling of the TCR-MHC-peptide complex

Amino acid sequences of TCRα and TCRβ were subjected to experiments to establish their predicted 3D structures based on homology modeling with amino acid sequences of HLA-A*24:02 and QYSPVQATF peptide on the TCRpMHCmodels,[42] TCRmodel,[41] and ImmuneScape[43] web servers. Generated PDB files or available files of crystal structures from PDB were assessed to calculate the interaction stability between TCR chains and MHC-peptide chains by using the PRODIGY[44] web server.

TCR-T cell culture

$CD14^-$ (or sometimes isolated $CD8^+$ were added) PBMCs (1×10^6/well on 24-well plates) were activated by Dynabeads Human T-Activator CD3/CD28 (Veritas, Tokyo, Japan) (cells/beads ratio = 2) for 3 days in the presence of IL-2, IL-7, and IL-15. Activated PBMCs were harvested, and lentiviral transduction was consecutively performed on days 3 and 4. The following day, magnetic beads were removed and further cultured for expansion. For the rapid expansion protocol, 30-Gy-irradiated allogeneic PBMCs from three donors were added (5–10:1 ratio) with 30 ng/mL anti-CD3 (OKT-3) antibody. In addition, fresh IL-2-, IL-7-, and IL-15-containing medium was added every 2–3 days over 10 days to maintain cell growth. A few days before analysis, TCR-transduced cells were labeled by biotin anti-mouse TCRb (H57-597) (BioLegend), followed by MACS enrichment using anti-biotin MicroBeads (Miltenyi Biotec).

Flow cytometry-based *in vitro* killing assay

Target cells were labeled by 5 μM CellTrace Violet (CTV) Cell Proliferation Kit (Invitrogen) in PBS for 15–20 min at 37°C. Then, 1×10^4 CTV-labeled target MM cells were cocultured with the indicated ratio of effector T cells for 18–24 h in 96-well round-bottom plates. After 1 μM TO-PRO-3 iodide (Invitrogen) staining, the cells were analyzed by Canto II, and $CTV^+TO\text{-}PRO\text{-}3^+$ cells in total CTV^+ cells were measured as percentages of dead cells. Cytotoxicity (percent) was calculated as ([effector + target] – [target only])/(100 – [target only]). For the peptide titration assay, CTV-labeled C1R-A*24:02 cells were pulsed with 9-mer peptide for 2 h at 37°C. 1×10^4 CTV-labeled, peptide-pulsed target C1R-A*24:02 cells were cocultured with 3×10^4 effector T cells for 18–24 h. Specific killing (percent) was calculated as the percentage of dead ([peptide-pulsed C1R-A*24:02 cells] – [DMSO-pulsed C1R-A*24:02 cells]). PHA-blasts were induced from PBMCs by stimulation with 3 μg/mL PHA-L and 100 U/mL IL-2 for 3 or 4 days.

Human MM cell xenograft antitumor model

Six-week-old female non-obese diabetic (NOD)/Shi-severe combined immunodeficiency (SCID), IL-2Rγ knockout (KO) Jic (NOG) mice were purchased from the Central Institute for Experimental Animals (Kawasaki, Kanagawa, Japan). All mice were maintained under specific pathogen-free conditions and studied in compliance with our institutional guidelines. KMS-11 cells were retrovirally transduced to express Akaluc-TdTomato[65] and purified twice by FACS Aria 3 cell sorter. 2×10^6 KMS-11-Akaluc-TdTomato cells were intravenously injected. Three days after the tumor injection, bioluminescence was measured by IVIS and randomized by the bioluminescence values. Next, 10×10^6 TCR-T cells were intravenously injected on days 3 and 7. In addition, 100 U/mouse IL-2, 50 ng/mouse IL-7, and 50 ng/mouse IL-15 were intraperitoneally injected on days 3, 4, 7, and 8 to maintain transferred T cells.

Study design

Almost all experiments performed in this study had at least two replicates to show biological reproducibility. The values from every experiment were pooled for statistical analysis, and each value and sample number are indicated in most figures. The study was not blinded; no statistical methods were used to predetermine the sample number.

Ethics approval

This study was conducted according to the guidelines of and approved by the ethical review board of RIKEN. Participants gave informed consent.

Statistical analysis

Graphs were generated and statistical analyses were performed using Microsoft Excel 2016 and R (3.6.1). For parametric data, an unpaired Student's t test was used. For non-parametric data, a Mann-Whitney U test was used. A log rank test was used for survival analysis. $p < 0.05$ was considered statistically significant and is indicated as follows: $^*p < 0.05$, $^{**}p < 0.01$, $^{***}p < 0.001$.

DATA AVAILABILITY

Data shown in this study are available upon reasonable request from the corresponding author.

SUPPLEMENTAL INFORMATION

Supplemental information can be found online at https://doi.org/10.1016/j.omtm.2023.05.014.

ACKNOWLEDGMENTS

We thank Shogo Ueda, An Sanpei, Yuya Hirahara, and Tomonori Iyoda for assistance and support in this study. We would also like to thank Drs. Hiroyuki Hata (Kumamoto University) and Masaki Yasukawa (Ehime University) for kindly providing MM cell lines. This work was supported by a JSPS KAKENHI Grant-in-Aid for Early-Career Scientists (JP21K16278) and Grant-in-Aid for Scientific Research (C) (JP19K07653).

AUTHOR CONTRIBUTIONS

M.O. conceived and designed the study after a discussion with K.S. and S.F., performed most of the experiments, and wrote and edited the manuscript with input from all authors. K.S. interpreted the data and wrote, reviewed, and edited the manuscript. H.N. helped with method development. S.Y. helped with material preparation and advice on the study. S.F. conceived, designed, and supervised the study and wrote, reviewed, and edited the manuscript. All authors have read and agreed to the final version of the manuscript.

DECLARATION OF INTERESTS

The authors declare no competing interests.

REFERENCES

1. Le, D.T., Durham, J.N., Smith, K.N., Wang, H., Bartlett, B.R., Aulakh, L.K., Lu, S., Kemberling, H., Wilt, C., Luber, B.S., et al. (2017). Mismatch repair deficiency predicts response of solid tumors to PD-1 blockade. Science *357*, 409–413. https://doi.org/10.1126/science.aan6733.

2. Litchfield, K., Reading, J.L., Puttick, C., Thakkar, K., Abbosh, C., Bentham, R., Watkins, T.B.K., Rosenthal, R., Biswas, D., Rowan, A., et al. (2021). Meta-analysis

of tumor- and T cell-intrinsic mechanisms of sensitization to checkpoint inhibition. Cell *184*, 596–614.e14. https://doi.org/10.1016/j.cell.2021.01.002.

3. Veatch, J.R., Singhi, N., Jesernig, B., Paulson, K.G., Zalevsky, J., Iaccucci, E., Tykodi, S.S., and Riddell, S.R. (2020). Mobilization of pre-existing polyclonal T cells specific to neoantigens but not self-antigens during treatment of a patient with melanoma with bempegaldesleukin and nivolumab. J. Immunother. Cancer *8*, e001591. https://doi.org/10.1136/jitc-2020-001591.

4. Okada, M., Shimizu, K., Iyoda, T., Ueda, S., Shinga, J., Mochizuki, Y., Watanabe, T., Ohara, O., and Fujii, S. (2020). PD-L1 expression affects neoantigen presentation. iScience *23*, 101238. https://doi.org/10.1016/j.isci.2020.101238.

5. Fritah, H., Rovelli, R., Chiang, C.L.-L., and Kandalaft, L.E. (2022). The current clinical landscape of personalized cancer vaccines. Cancer Treat Rev. *106*, 102383. https://doi.org/10.1016/j.ctrv.2022.102383.

6. Zacharakis, N., Chinnasamy, H., Black, M., Xu, H., Lu, Y.-C., Zheng, Z., Pasetto, A., Langhan, M., Shelton, T., Prickett, T., et al. (2018). Immune recognition of somatic mutations leading to complete durable regression in metastatic breast cancer. Nat. Med. *24*, 724–730. https://doi.org/10.1038/s41591-018-0040-8.

7. van den Berg, J.H., Heemskerk, B., van Rooij, N., Gomez-Eerland, R., Michels, S., van Zon, M., de Boer, R., Bakker, N.A.M., Jorritsma-Smit, A., van Buuren, M.M., et al. (2020). Tumor infiltrating lymphocytes (TIL) therapy in metastatic melanoma: boosting of neoantigen-specific T cell reactivity and long-term follow-up. J. Immunother. Cancer *8*, e000848. https://doi.org/10.1136/jitc-2020-000848.

8. Kristensen, N.P., Heeke, C., Tvingsholm, S.A., Borch, A., Draghi, A., Crowther, M.D., Carri, I., Munk, K.K., Holm, J.S., Bjerregaard, A.-M., et al. (2022). Neoantigen-reactive CD8+ T cells affect clinical outcome of adoptive cell therapy with tumor-infiltrating lymphocytes in melanoma. J. Clin. Invest. *132*, e150535. https://doi.org/10.1172/JCI150535.

9. Okada, M., Shimizu, K., and Fujii, S. (2022). Identification of neoantigens in cancer cells as targets for immunotherapy. Int. J. Mol. Sci. *23*, 2594. https://doi.org/10.3390/ijms23052594.

10. Zhou, W., Yu, J., Li, Y., and Wang, K. (2022). Neoantigen-specific TCR-T cell-based immunotherapy for acute myeloid leukemia. Exp. Hematol. Oncol. *11*, 100. https://doi.org/10.1186/s40164-022-00353-3.

11. Palumbo, A., and Anderson, K. (2011). Multiple myeloma. N. Engl. J. Med. *364*, 1046–1060. https://doi.org/10.1056/NEJMra1011442.

12. Iyoda, T., Yamasaki, S., Hidaka, M., Kawano, F., Abe, Y., Suzuki, K., Kadowaki, N., Shimizu, K., and Fujii, S. (2018). Amelioration of NK cell function driven by Vα24+ invariant NKT cell activation in multiple myeloma. Clin. Immunol. *187*, 76–84. https://doi.org/10.1016/j.clim.2017.10.007.

13. Cowan, A.J., Allen, C., Barac, A., Basaleem, H., Bensenor, I., Curado, M.P., Foreman, K., Gupta, R., Harvey, J., Hosgood, H.D., et al. (2018). Global burden of multiple myeloma: a systematic analysis for the global burden of disease study 2016. JAMA Oncol. *4*, 1221–1227. https://doi.org/10.1001/jamaoncol.2018.2128.

14. Lesch, S., and Gill, S. (2021). The promise and perils of immunotherapy. Blood Adv. *5*, 3709–3725. https://doi.org/10.1182/bloodadvances.2021004453C.

15. van de Donk, N.W., Pawlyn, C., and Yong, K.L. (2021). Multiple myeloma. Lancet *397*, 410–427. https://doi.org/10.1016/S0140-6736(21)00135-5.

16. Podar, K., and Leleu, X. (2021). Relapsed/refractory multiple myeloma in 2020/2021 and beyond. Cancers *13*, 5154. https://doi.org/10.3390/cancers13205154.

17. Perumal, D., Imai, N., Laganà, A., Finnigan, J., Melnekoff, D., Leshchenko, V.V., Solovyov, A., Madduri, D., Chari, A., Cho, H.J., et al. (2020). Mutation-derived neoantigen-specific T-cell responses in multiple myeloma. Clin. Cancer Res. *26*, 450–464. https://doi.org/10.1158/1078-0432.CCR-19-2309.

18. Miller, A., Asmann, Y., Cattaneo, L., Braggio, E., Keats, J., Auclair, D., Lonial, S., MMRF CoMMpass Network, Russell, S.J., and Stewart, A.K. (2017). High somatic mutation and neoantigen burden are correlated with decreased progression-free survival in multiple myeloma. Blood Cancer J. *7*, e612. https://doi.org/10.1038/bcj.2017.94.

19. Dong, C., Cesarano, A., Bombaci, G., Reiter, J.L., Yu, C.Y., Wang, Y., Jiang, Z., Zaid, M.A., Huang, K., Lu, X., et al. (2021). Intron retention-induced neoantigen load correlates with unfavorable prognosis in multiple myeloma. Oncogene *40*, 6130–6138. https://doi.org/10.1038/s41388-021-02005-y.

20. Badros, A., Hyjek, E., Ma, N., Lesokhin, A., Dogan, A., Rapoport, A.P., Kocoglu, M., Lederer, E., Philip, S., Milliron, T., et al. (2017). Pembrolizumab, pomalidomide, and low-dose dexamethasone for relapsed/refractory multiple myeloma. Blood *130*, 1189–1197. https://doi.org/10.1182/blood-2017-03-775122.

21. D'Souza, A., Hari, P., Pasquini, M., Braun, T., Johnson, B., Lundy, S., Couriel, D., Hamadani, M., Magenau, J., Dhakal, B., et al. (2019). A phase 2 study of pembrolizumab during lymphodepletion after autologous hematopoietic cell transplantation for multiple myeloma. Biol. Blood Marrow Transplant. *25*, 1492–1497. https://doi.org/10.1016/j.bbmt.2019.04.005.

22. Mateos, M.-V., Blacklock, H., Schjesvold, F., Oriol, A., Simpson, D., George, A., Goldschmidt, H., Larocca, A., Chanan-Khan, A., Sherbenou, D., et al. (2019). Pembrolizumab plus pomalidomide and dexamethasone for patients with relapsed or refractory multiple myeloma (KEYNOTE-183): a randomised, open-label, phase 3 trial. Lancet. Haematol. *6*, e459–e469. https://doi.org/10.1016/S2352-3026(19)30110-3.

23. Kwon, M., Kim, C.G., Lee, H., Cho, H., Kim, Y., Lee, E.C., Choi, S.J., Park, J., Seo, I.-H., Bogen, B., et al. (2020). PD-1 blockade reinvigorates bone marrow CD8+ T cells from patients with multiple myeloma in the presence of TGFβ inhibitors. Clin. Cancer Res. *26*, 1644–1655. https://doi.org/10.1158/1078-0432.CCR-19-0267.

24. Zelle-Rieser, C., Thangavadivel, S., Biedermann, R., Brunner, A., Stoitzner, P., Willenbacher, E., Greil, R., and Jöhrer, K. (2016). T cells in multiple myeloma display features of exhaustion and senescence at the tumor site. J. Hematol. Oncol. *9*, 116. https://doi.org/10.1186/s13045-016-0345-3.

25. Minnie, S.A., Kuns, R.D., Gartlan, K.H., Zhang, P., Wilkinson, A.N., Samson, L., Guillerey, C., Engwerda, C., MacDonald, K.P.A., Smyth, M.J., et al. (2018). Myeloma escape after stem cell transplantation is a consequence of T-cell exhaustion and is prevented by TIGIT blockade. Blood *132*, 1675–1688. https://doi.org/10.1182/blood-2018-01-825240.

26. Strønen, E., Toebes, M., Kelderman, S., van Buuren, M.M., Yang, W., van Rooij, N., Donia, M., Böschen, M.L., Lund-Johansen, F., Olweus, J., and Schumacher, T.N. (2016). Targeting of cancer neoantigens with donor-derived T cell receptor repertoires. Science *352*, 1337–1341. https://doi.org/10.1126/science.aaf2288.

27. van der Lee, D.I., Reijmers, R.M., Honders, M.W., Hagedoorn, R.S., de Jong, R.C., Kester, M.G., van der Steen, D.M., de Ru, A.H., Kweekel, C., Bijen, H.M., et al. (2019). Mutated nucleophosmin 1 as immunotherapy target in acute myeloid leukemia. J. Clin. Invest. *129*, 774–785. https://doi.org/10.1172/JCI97482.

28. Wei, T., Leisegang, M., Xia, M., Kiyotani, K., Li, N., Zeng, C., Deng, C., Jiang, J., Harada, M., Agrawal, N., et al. (2021). Generation of neoantigen-specific T cells for adoptive cell transfer for treating head and neck squamous cell carcinoma. OncoImmunology *10*, 1929726. https://doi.org/10.1080/2162402X.2021.1929726.

29. Leidner, R., Sanjuan Silva, N., Huang, H., Sprott, D., Zheng, C., Shih, Y.-P., Leung, A., Payne, R., Sutcliffe, K., Cramer, J., et al. (2022). Neoantigen T-cell receptor gene therapy in pancreatic cancer. N. Engl. J. Med. *386*, 2112–2119. https://doi.org/10.1056/NEJMoa2119662.

30. Kim, S.P., Vale, N.R., Zacharakis, N., Krishna, S., Yu, Z., Gasmi, B., Gartner, J.J., Sindiri, S., Malekzadeh, P., Deniger, D.C., et al. (2022). Adoptive cellular therapy with autologous tumor-infiltrating lymphocytes and T-cell receptor-engineered T cells targeting common p53 neoantigens in human solid tumors. Cancer Immunol. Res. *10*, 932–946. https://doi.org/10.1158/2326-6066.CIR-22-0040.

31. Rapoport, A.P., Stadtmauer, E.A., Binder-Scholl, G.K., Goloubeva, O., Vogl, D.T., Lacey, S.F., Badros, A.Z., Garfall, A., Weiss, B., Finklestein, J., et al. (2015). NY-ESO-1-specific TCR-engineered T cells mediate sustained antigen-specific antitumor effects in myeloma. Nat. Med. *21*, 914–921. https://doi.org/10.1038/nm.3910.

32. Mehdi, S.H., Nafees, S., Mehdi, S.J., Morris, C.A., Mashouri, L., and Yoon, D. (2021). Animal models of multiple myeloma bone disease. Front. Genet. *12*, 640954. https://doi.org/10.3389/fgene.2021.640954.

33. Ghandi, M., Huang, F.W., Jané-Valbuena, J., Kryukov, G.V., Lo, C.C., McDonald, E.R., Barretina, J., Gelfand, E.T., Bielski, C.M., Li, H., et al. (2019). Next-generation characterization of the cancer cell line Encyclopedia. Nature *569*, 503–508. https://doi.org/10.1038/s41586-019-1186-3.

34. Togawa, A., Inoue, N., Miyamoto, K., Hyodo, H., and Namba, M. (1982). Establishment and characterization of a human myeloma cell line (KMM-1). Int. J. Cancer *29*, 495–500. https://doi.org/10.1002/ijc.2910290502.

35. Shimizu, K., Iyoda, T., Sanpei, A., Nakazato, H., Okada, M., Ueda, S., Kato-Murayama, M., Murayama, K., Shirouzu, M., Harada, N., et al. (2021). Identification of TCR repertoires in functionally competent cytotoxic T cells cross-reactive to SARS-CoV-2. Commun. Biol. *4*, 1365. https://doi.org/10.1038/s42003-021-02885-6.

36. Ikeda, M., Okusaka, T., Ohno, I., Mitsunaga, S., Kondo, S., Ueno, H., Morizane, C., Gemmoto, K., Suna, H., Ushida, Y., and Furuse, J. (2021). Phase I studies of peptide vaccine cocktails derived from GPC3, WDRPUH and NEIL3 for advanced hepatocellular carcinoma. Immunotherapy *13*, 371–385. https://doi.org/10.2217/imt-2020-0278.

37. Jurtz, V., Paul, S., Andreatta, M., Marcatili, P., Peters, B., and Nielsen, M. (2017). NetMHCpan-4.0: improved peptide-MHC class I interaction predictions integrating eluted ligand and peptide binding affinity data. J. Immunol. *199*, 3360–3368. https://doi.org/10.4049/jimmunol.1700893.

38. Dash, P., Fiore-Gartland, A.J., Hertz, T., Wang, G.C., Sharma, S., Souquette, A., Crawford, J.C., Clemens, E.B., Nguyen, T.H.O., Kedzierska, K., et al. (2017). Quantifiable predictive features define epitope-specific T cell receptor repertoires. Nature *547*, 89–93. https://doi.org/10.1038/nature22383.

39. Marcu, A., Schlosser, A., Keupp, A., Trautwein, N., Johann, P., Wölfl, M., Lager, J., Monoranu, C.M., Walz, J.S., Henkel, L.M., et al. (2021). Natural and cryptic peptides dominate the immunopeptidome of atypical teratoid rhabdoid tumors. J. Immunother. Cancer *9*, e003404. https://doi.org/10.1136/jitc-2021-003404.

40. Hirama, T., Tokita, S., Nakatsugawa, M., Murata, K., Nannya, Y., Matsuo, K., Inoko, H., Hirohashi, Y., Hashimoto, S., Ogawa, S., et al. (2021). Proteogenomic identification of an immunogenic HLA class I neoantigen in mismatch repair-deficient colorectal cancer tissue. JCI Insight *6*, e146356. https://doi.org/10.1172/jci.insight.146356.

41. Gowthaman, R., and Pierce, B.G. (2018). TCRmodel: high resolution modeling of T cell receptors from sequence. Nucleic Acids Res. *46*, W396–W401. https://doi.org/10.1093/nar/gky432.

42. Jensen, K.K., Rantos, V., Jappe, E.C., Olsen, T.H., Jespersen, M.C., Jurtz, V., Jessen, L.E., Lanzarotti, E., Mahajan, S., Peters, B., et al. (2019). TCRpMHCmodels: structural modelling of TCR-pMHC class I complexes. Sci. Rep. *9*, 14530. https://doi.org/10.1038/s41598-019-50932-4.

43. Li, S., Wilamowski, J., Teraguchi, S., van Eerden, F.J., Rozewicki, J., Davila, A., Xu, Z., Katoh, K., and Standley, D.M. (2019). Structural modeling of lymphocyte receptors and their antigens. Methods Mol. Biol. *2048*, 207–229. https://doi.org/10.1007/978-1-4939-9728-2_17.

44. Xue, L.C., Rodrigues, J.P., Kastritis, P.L., Bonvin, A.M., and Vangone, A. (2016). PRODIGY: a web server for predicting the binding affinity of protein-protein complexes. Bioinformatics *32*, 3676–3678. https://doi.org/10.1093/bioinformatics/btw514.

45. Cohen, C.J., Zhao, Y., Zheng, Z., Rosenberg, S.A., and Morgan, R.A. (2006). Enhanced antitumor activity of murine-human hybrid T-cell receptor (TCR) in human lymphocytes is associated with improved pairing and TCR/CD3 stability. Cancer Res. *66*, 8878–8886. https://doi.org/10.1158/0008-5472.CAN-06-1450.

46. Kirtane, K., Elmariah, H., Chung, C.H., and Abate-Daga, D. (2021). Adoptive cellular therapy in solid tumor malignancies: review of the literature and challenges ahead. J. Immunother. Cancer *9*, e002723. https://doi.org/10.1136/jitc-2021-002723.

47. Cho, H.-I., Kim, U.-H., Shin, A.-R., Won, J.-N., Lee, H.-J., Sohn, H.-J., and Kim, T.-G. (2018). A novel Epstein-Barr virus-latent membrane protein-1-specific T-cell receptor for TCR gene therapy. Br. J. Cancer *118*, 534–545. https://doi.org/10.1038/bjc.2017.475.

48. Bilich, T., Nelde, A., Bauer, J., Walz, S., Roerden, M., Salih, H.R., Weisel, K., Besemer, B., Marcu, A., Lübke, M., et al. (2020). Mass spectrometry-based identification of a B-cell maturation antigen-derived T-cell epitope for antigen-specific immunotherapy of multiple myeloma. Blood Cancer J. *10*, 24. https://doi.org/10.1038/s41408-020-0288-3.

49. Little, P., Jo, H., Hoyle, A., Mazul, A., Zhao, X., Salazar, A.H., Farquhar, D., Sheth, S., Masood, M., Hayward, M.C., et al. (2021). UNMASC: tumor-only variant calling with unmatched normal controls. NAR Cancer *3*, zcab040. https://doi.org/10.1093/narcan/zcab040.

50. McLaughlin, R.T., Asthana, M., Di Meo, M., Ceccarelli, M., Jacob, H.J., and Masica, D.L. (2023). Fast, accurate, and racially unbiased pan-cancer tumor-only variant calling with tabular machine learning. NPJ Precis. Oncol. *7*, 4. https://doi.org/10.1038/s41698-022-00340-1.

51. Manier, S., Salem, K.Z., Park, J., Landau, D.A., Getz, G., and Ghobrial, I.M. (2017). Genomic complexity of multiple myeloma and its clinical implications. Nat. Rev. Clin. Oncol. *14*, 100–113. https://doi.org/10.1038/nrclinonc.2016.122.

52. Hoang, P.H., Cornish, A.J., Sherborne, A.L., Chubb, D., Kimber, S., Jackson, G., Morgan, G.J., Cook, G., Kinnersley, B., Kaiser, M., and Houlston, R.S. (2020). An enhanced genetic model of relapsed IGH-translocated multiple myeloma evolutionary dynamics. Blood Cancer J. *10*, 101. https://doi.org/10.1038/s41408-020-00367-2.

53. He, H., Li, Z., Lu, J., Qiang, W., Jiang, S., Xu, Y., Fu, W., Zhai, X., Zhou, L., Qian, M., and Du, J. (2022). Single-cell RNA-seq reveals clonal diversity and prognostic genes of relapsed multiple myeloma. Clin. Transl. Med. *12*, e757. https://doi.org/10.1002/ctm2.757.

54. Merz, M., Merz, A.M.A., Wang, J., Wei, L., Hu, Q., Hutson, N., Rondeau, C., Celotto, K., Belal, A., Alberico, R., et al. (2022). Deciphering spatial genomic heterogeneity at a single cell resolution in multiple myeloma. Nat. Commun. *13*, 807. https://doi.org/10.1038/s41467-022-28266-z.

55. Dutta, A.K., Fink, J.L., Grady, J.P., Morgan, G.J., Mullighan, C.G., To, L.B., Hewett, D.R., and Zannettino, A.C.W. (2019). Subclonal evolution in disease progression from MGUS/SMM to multiple myeloma is characterised by clonal stability. Leukemia *33*, 457–468. https://doi.org/10.1038/s41375-018-0206-x.

56. Bailur, J.K., McCachren, S.S., Doxie, D.B., Shrestha, M., Pendleton, K., Nooka, A.K., Neparidze, N., Parker, T.L., Bar, N., Kaufman, J.L., et al. (2019). Early alterations in stem-like/resident T cells, innate and myeloid cells in the bone marrow in preneoplastic gammopathy. JCI Insight *5*, 127807. https://doi.org/10.1172/jci.insight.127807.

57. Schinke, C., Poos, A.M., Bauer, M., John, L., Johnson, S., Deshpande, S., Carrillo, L., Alapat, D., Rasche, L., Thanendrarajan, S., et al. (2022). Characterizing the role of the immune microenvironment in multiple myeloma progression at a single-cell level. Blood Adv. *6*, 5873–5883. https://doi.org/10.1182/bloodadvances.2022007217.

58. Okada, M., Chikuma, S., Kondo, T., Hibino, S., Machiyama, H., Yokosuka, T., Nakano, M., and Yoshimura, A. (2017). Blockage of core fucosylation reduces cell-surface expression of PD-1 and promotes anti-tumor immune responses of T cells. Cell Rep. *20*, 1017–1028. https://doi.org/10.1016/j.celrep.2017.07.027.

59. Iriguchi, S., Yasui, Y., Kawai, Y., Arima, S., Kunitomo, M., Sato, T., Ueda, T., Minagawa, A., Mishima, Y., Yanagawa, N., et al. (2021). A clinically applicable and scalable method to regenerate T-cells from iPSCs for off-the-shelf T-cell immunotherapy. Nat. Commun. *12*, 430. https://doi.org/10.1038/s41467-020-20658-3.

60. Giudicelli, V., Brochet, X., and Lefranc, M.-P. (2011). IMGT/V-QUEST: IMGT standardized analysis of the immunoglobulin (IG) and T cell receptor (TR) nucleotide sequences. Cold Spring Harb. Protoc. *2011*, 695–715. https://doi.org/10.1101/pdb.prot5633.

61. Dobin, A., Davis, C.A., Schlesinger, F., Drenkow, J., Zaleski, C., Jha, S., Batut, P., Chaisson, M., and Gingeras, T.R. (2013). STAR: ultrafast universal RNA-seq aligner. Bioinformatics *29*, 15–21. https://doi.org/10.1093/bioinformatics/bts635.

62. Van der Auwera, G.A., Carneiro, M.O., Hartl, C., Poplin, R., Del Angel, G., Levy-Moonshine, A., Jordan, T., Shakir, K., Roazen, D., Thibault, J., et al. (2013). From FastQ data to high confidence variant calls: the Genome Analysis Toolkit best practices pipeline. Curr. Protoc. Bioinformatics *43*, 11.10.1–11.10.33. https://doi.org/10.1002/0471250953.bi1110s43.

63. Koboldt, D.C., Zhang, Q., Larson, D.E., Shen, D., McLellan, M.D., Lin, L., Miller, C.A., Mardis, E.R., Ding, L., and Wilson, R.K. (2012). VarScan 2: somatic mutation and copy number alteration discovery in cancer by exome sequencing. Genome Res. *22*, 568–576. https://doi.org/10.1101/gr.129684.111.

64. Orenbuch, R., Filip, I., Comito, D., Shaman, J., Pe'er, I., and Rabadan, R. (2020). arcasHLA: high-resolution HLA typing from RNAseq. Bioinformatics *36*, 33–40. https://doi.org/10.1093/bioinformatics/btz474.

65. Iwano, S., Sugiyama, M., Hama, H., Watakabe, A., Hasegawa, N., Kuchimaru, T., Tanaka, K.Z., Takahashi, M., Ishida, Y., Hata, J., et al. (2018). Single-cell bioluminescence imaging of deep tissue in freely moving animals. Science *359*, 935–939. https://doi.org/10.1126/science.aaq1067.